

Methodological demonstration of laser beam pointing control for space gravitational wave detection missions

Yu-Hui Dong, He-Shan Liu, Zi-Ren Luo, Yu-Qiong Li, and Gang Jin

Citation: [Review of Scientific Instruments](#) **85**, 074501 (2014); doi: 10.1063/1.4891037

View online: <http://dx.doi.org/10.1063/1.4891037>

View Table of Contents: <http://scitation.aip.org/content/aip/journal/rsi/85/7?ver=pdfcov>

Published by the [AIP Publishing](#)

Articles you may be interested in

[Tip-tilt mirror suspension: Beam steering for advanced laser interferometer gravitational wave observatory sensing and control signals](#)

Rev. Sci. Instrum. **82**, 125108 (2011); 10.1063/1.3669532

[Characterization of wave-front corrected 100 TW, 10 Hz laser pulses with peak intensities greater than 10 20 W/cm²](#)

Rev. Sci. Instrum. **77**, 023102 (2006); 10.1063/1.2166669

[First adaptive optics control of laser beam based on interferometric phase-front detection](#)

Rev. Sci. Instrum. **76**, 083119 (2005); 10.1063/1.2010625

[Laser Spot Size Control In Space](#)

AIP Conf. Proc. **664**, 571 (2003); 10.1063/1.1582143

[Adaptive optics approach for prefiltering of geometrical fluctuations of the input laser beam of an interferometric gravitational waves detector](#)

Rev. Sci. Instrum. **74**, 2570 (2003); 10.1063/1.1537043



Not all AFMs are created equal
Asylum Research Cypher™ AFMs
There's no other AFM like Cypher

www.AsylumResearch.com/NoOtherAFMLikeIt

OXFORD
INSTRUMENTS
The Business of Science®

Methodological demonstration of laser beam pointing control for space gravitational wave detection missions

Yu-Hui Dong,^{1,2,a)} He-Shan Liu,^{1,2,a)} Zi-Ren Luo,¹ Yu-Qiong Li,¹ and Gang Jin^{1,b)}

¹National Microgravity Laboratory (NML), Institute of Mechanics, Chinese Academy of Sciences, Beijing 100190, People's Republic of China

²University of Chinese Academy of Sciences, Beijing 100190, People's Republic of China

(Received 16 April 2014; accepted 12 July 2014; published online 29 July 2014)

In space laser interferometer gravitational wave (G.W.) detection missions, the stability of the laser beam pointing direction has to be kept at $10 \text{ nrad}/\sqrt{\text{Hz}}$. Otherwise, the beam pointing jitter noise will dominate the noise budget and make the detection of G.W. impossible. Disturbed by the residue non-conservative forces, the fluctuation of the laser beam pointing direction could be a few $\mu\text{rad}/\sqrt{\text{Hz}}$ at frequencies from 0.1 mHz to 10 Hz. Therefore, the laser beam pointing control system is an essential requirement for those space G.W. detection missions. An on-ground test of such beam pointing control system is performed, where the Differential Wave-front Sensing technique is used to sense the beams pointing jitter. An active controlled steering mirror is employed to adjust the beam pointing direction to compensate the jitter. The experimental result shows that the pointing control system can be used for very large dynamic range up to $5 \mu\text{rad}$. At the interested frequencies of space G.W. detection missions, between 1 mHz and 1 Hz, beam pointing stability of $6 \text{ nrad}/\sqrt{\text{Hz}}$ is achieved.

© 2014 AIP Publishing LLC. [<http://dx.doi.org/10.1063/1.4891037>]

I. INTRODUCTION

Driven by various motivations, many space missions are proposed to use the laser interferometer to detect and observe gravitational wave (G.W.) in the past 20 years.¹⁻⁶ The most interesting G.W. frequency band covered by those space missions is from 0.1 mHz to 10 Hz and the corresponding working baselines of those space interferometers are ranging from a few hundred thousand kilometers to several million kilometers. Among all the technical difficulties in long baseline space laser metrology, such as weak light phase lock, laser frequency noise suppression, and ultra-stable oscillator noise cancelation, the problem of the laser beam pointing control is the most stringent one.⁷⁻¹⁰

For example, the laser beam pointing control is the key to the evolved Laser Interferometer Space Antenna (eLISA). The eLISA mission is a self-funded space G.W. detection project of European Space Agency (ESA). If launched, the eLISA can be expected to confront the G.W. predicted by Einstein's General Relativity, and it will open up a new window for the observation of the universe.^{3,11-14} Its predecessor is Laser Interferometer Space Antenna (LISA).¹ The eLISA is planning to launch three satellites, one mother satellite and two daughter satellites. The three satellites, separated by $1 \times 10^6 \text{ km}$, form a huge equilateral triangle with the center of the formation lying in ecliptic plane 1 AU from the Sun and 20° behind the Earth. The mother satellite will send one laser beam to each daughter satellite, the light will be received and phase locked by daughter satellites, and then each daughter satellite will send one laser beam back to mother satellite to form a Michelson type interferometer.^{2,14,15}

To achieve the scientific objectives, the sensitivity of eLISA should be better than $12 \text{ pm}/\sqrt{\text{Hz}}$ in the measurement band of 1 mHz-1 Hz.¹⁴ The beam pointing jitter noise is expected to be one of the most prominent optical-path noise.^{1,7,8} The spacecraft jitter caused by the non-conservative forces, such as solar wind, solar radiation, cosmic rays, etc., can be suppressed by the disturbance reduction system.^{16,17} But the residual attitude dynamics of the spacecraft and the Proof Mass will even result in the jitter of transmitting light. After $1 \times 10^6 \text{ km}$ spreading, the transmitting light received by local spacecraft is mixed with local laser and the beat-note signal is detected by the photo-detector. The angular jitter of the transmitting light will cause phase noise due to the geometrical distortion of the transmitting telescope. The apparent phase noise $\delta\varphi$ in the far field can be showed as^{1,7,8}

$$\delta\varphi = \frac{1}{32} \left(\frac{2\pi}{\lambda} \right)^3 d D^2 \theta_{\text{dc}} \delta\theta, \quad (1)$$

where θ_{dc} is the static offset error in the pointing, $\delta\theta$ is the pointing jitter, D is diameter of telescope, d is amplitude of curvature error in the wave-front caused by the geometrical distortion of the transmitting telescope, and λ is laser wavelength. Over $1 \times 10^6 \text{ km}$, the laser beam pointing direction θ_{dc} have to be aligned as precise as 20 nrad , and the variation of the alignment $\delta\theta$ should be kept no more than $10 \text{ nrad}/\sqrt{\text{Hz}}$ at the frequencies from 1 mHz and 1 Hz.² Otherwise, the beam pointing jitter noise will dominate the displacement noise budget of interferometric measurement system and make the detection of G.W. impossible. The influence of complex cosmic background makes the requirement of the beam pointing stability hard to achieve and the weak light about 100 pW because of $1 \times 10^6 \text{ km}$ transmitting makes the situation even worse.

a) Y.-H. Dong and H.-S. Liu contributed equally to this work.

b) Author to whom correspondence should be addressed. Electronic mail: gajin@imech.ac.cn.

To achieve the desired beam pointing stability, an active feed-back control system is essential. Two sets of such systems will be installed in mother satellite, and one set for each daughter satellite. Split by an unbalanced beam splitter, the local laser beam is divided into two parts: one part with most of the power will be sent to the remote satellite, the other with small part will be used for Differential Wave-front Sensing (DWS).^{18–23} DWS technique will be introduced in Sec. II. By interfering received laser beam with small part of local beam, this control system use DWS to measure the deviated angle between the pointing directions of two beams. This information will be sent to a controller which will command a piezoelectric transducer (PZT). The PZT then drives a steering mirror to adjust the pointing direction of local beam parallel to the pointing direction of received beam. Simultaneously, the local beam sent out to the remote satellite will travel along the same direction where the received beam comes.

Though it is an underdevelopment technology for space G.W. detection missions, such control system is not new for the eLISA's ground based counterparts.²¹ Since the mirrors used in ground based detectors are usually several kilograms, the coil-magnet system replaces PZT as actuator to adjust the mirrors. In the interested frequencies of ground based detectors, above 20 Hz, the pointing stability better than 1 nrad/ $\sqrt{\text{Hz}}$ can be achieved. However, in frequencies below 1 Hz, beam pointing fluctuation raise up quickly.²¹

Motivated by increasing interests of China in the field of space G.W. detection,^{3,24,25} a bench-top beam pointing control system for space G.W. detection mission is built and tested. Two PZTs are used in this bench-top experiment: one is to simulate pointing jitter of the incident beam; and the other is used for pointing control system to compensate the jitter. In space G.W. detection missions, the pointing jitter caused by residue non-conserved forces will be a few μrad .^{2,26} A 5 $\mu\text{rad}/\sqrt{\text{Hz}}$ single frequency jitter at 0.01 Hz is simulated as an input jitter. Under close-loop performance of the bench-top beam pointing control system, the pointing stability of 6 nrad/ $\sqrt{\text{Hz}}$ is achieved in interested frequencies of space G.W. detection missions. Moreover, this beam pointing control technique can also be used for possible future satellite gravity missions.^{27–31} In this article, the Amplitude Spectra Density (ASD) and Linearized Amplitude Spectra Density (LASD) are used to evaluate the performance of the pointing control system.³²

II. EXPERIMENT SETUPS

The laser beam pointing control system built on a bench-top can be separated into two functional parts (Fig. 1). In laser modulation bench, a 500 mW linear polarized single mode laser with wavelength of 1064 nm is split by a 50/50 beam splitter. Then two split beams are sent into two AOMs, and the offset frequency between two AOMs is 40 kHz. One of the laser beams is used to simulate the receiving laser while the other is used as the local laser. The two laser beams will be fiber-coupled and sent to ultra-stable optical bench. Each beam will be reflected by a steering mirror mounted on PZT. As shown in Fig. 2, a beam reflected by the mirror on the PZT (XMT XS-330.2SL) which is controlled by so-called

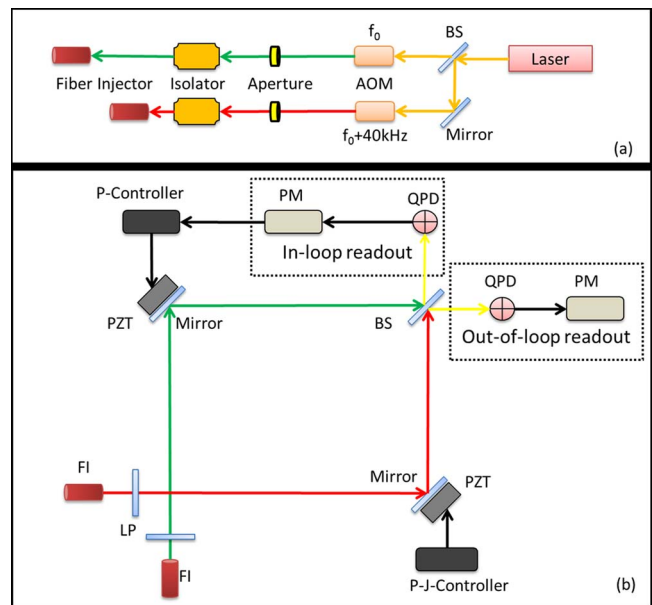


FIG. 1. Schematic diagram of the beam pointing control system: (a) laser modulation bench of the pointing control system; (b) ultra-stable optical bench of the pointing control system. Where AOM: acoustic-optical modulator, FI: fiber injector, BS: 50/50 beam splitter, LP: linear polarizer, P-J-Controller: pointing jitter controller, P-Controller: pointing controller, PM: phasemeter, QPD: quadrant photo detector.

P-J-controller is used to simulate beam pointing jitter of simulated receiving beam. The other PZT (PI s330.2 SL) controlled by P-controller is used for our beam pointing control system to adjust the local beam parallel to simulated receiving beam. The two beams will be interfered at a 50/50 beam-splitter and the relative angle between them will be read out by DWS technique. DWS consisting of a quadrant photo detector (QPD) and a phasemeter is a well-known technique for measuring the relative wave-front misalignment between two beams with high sensitivity,^{18–23} see Fig. 3. In small misalignment, the average phase difference $\Delta\theta$ between opposing halves of QPD can be approximated shown as^{27,29}

$$\Delta\theta \approx \frac{16r}{3\lambda} \cdot \alpha = k \cdot \alpha, \quad (2)$$

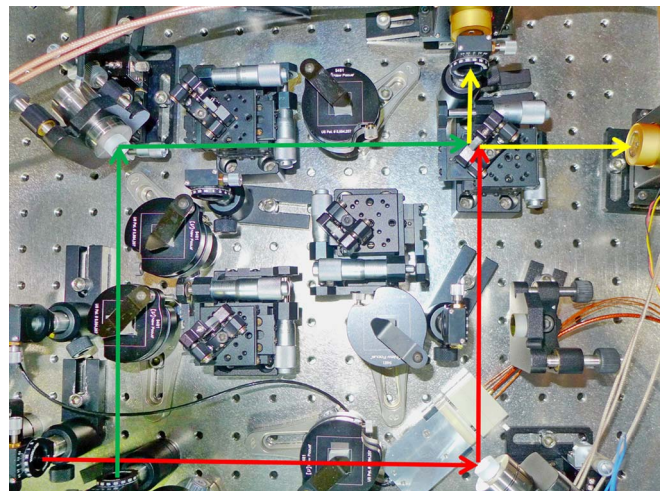


FIG. 2. Layout of the laser beam pointing control system.

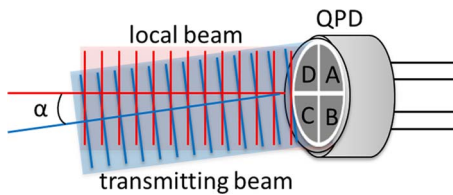


FIG. 3. Principle of DWS technique.

where α is the relative wave-front tilt, r is the beam radius, λ is the laser wavelength, and k is the conversion factor. Acquiring the real-time information of relative angles offered by in-loop readout, the beam pointing controller regulates the PI steering mirror (PI s330.2 SL) which drives the direction of the local laser to follow and lock the direction of the simulated receiving laser to improve the pointing stability. The real-time performance of the beam pointing control system is evaluated by out-of-loop readout.

III. CALIBRATION

In order to describe the pointing jitter of the received light, two degrees of freedom are required: where yaw motion presents the horizontal misalignment and pitch motion presents the vertical fluctuation.

The conversion factor k from geometrical angle to electrical phase difference, which can be predicted by DWS theory, should be initially calibrated by the experiment. The calibration curves of the steering mirror driven by PI PZT are shown in Fig. 4. The two freedoms are calibrated independently. When yaw (pitch) motion is steered from $-100 \mu\text{rad}$ to $100 \mu\text{rad}$, the pitch (yaw) motion is kept at zero. The dotted lines are the phase difference read out by DWS technique, and the solid lines are the linear regression lines of phase difference data. The correlation coefficient of the linear fittings for yaw and pitch motion is 0.999987 and 0.999981, respectively, which indicates a very good linearity between DWS signal and relative angles. The conversion factors for yaw and pitch motion can be obtained from linear fitting curve: $k_{\text{yaw}} \approx 5703 \text{ rad/rad}$ and $k_{\text{pitch}} \approx 4790 \text{ rad/rad}$, where k_{yaw} is the conversion factor of yaw axis rotation; k_{pitch} is the conversion factor of pitch axis rotation. The different amplitudes of the conversion factor may originate from various factors, such as imperfect overlapping of two interfering beams,

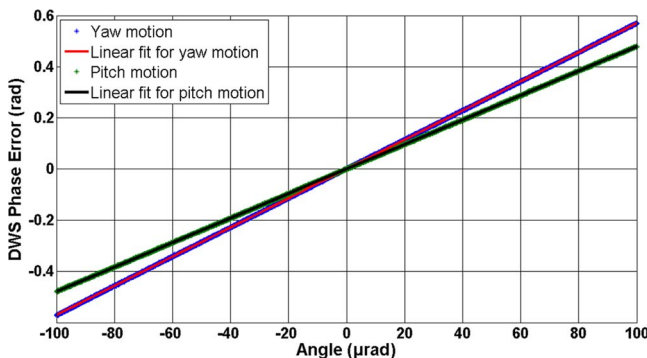


FIG. 4. Linear fit for yaw motion and pitch motion.

inhomogeneous spatial distribution of the phase, or non-perpendicularity between laser beams and photo-detector.

The readout noise caused by photo detector, bayonet nut connectors (BNCs), transmission line wire, and phasemeter is also calibrated. One simulated heterodyne signal is divided into four parts to represent four signals obtained from the QPD. Through BNC and transmission wires, the four divided parts will be sent into phasemeter to calculate the phase difference between opposing halves of QPD. Dividing the phase difference with the conversion factor we have DWS signals. If photo detector, BNCs, wires, and phasemeter are noise free, the output DWS signals should be zero. But practically there are always some noises.

The readout noises of yaw and pitch motion are calibrated independently, and the data are shown in ASD diagram, see in Fig. 5. The solid curves are LASD data of yaw and pitch. The readout noise levels for yaw and pitch over the frequency band 1 mHz-1 Hz are: $\alpha_{\text{yaw}} \approx 2 \text{ nrad}/\sqrt{\text{Hz}}$ and $\alpha_{\text{pitch}} \approx 2.3 \text{ nrad}/\sqrt{\text{Hz}}$. The different noise levels in yaw and pitch are mainly caused by the different conversion factors.

IV. RESULTS AND DISCUSSIONS

During the experiment, the P-J-controller commands on XMT steering mirror to rotate around yaw and pitch axis simultaneously. In order to simulate the situation of eLISA, the amplitudes of modulated pointing jitters, both yaw and pitch, are set to $5 \mu\text{rad}/\sqrt{\text{Hz}}$. For simplicity, the frequency of simulated jitter is fixed at 10 mHz. The P-controller will drive PI steering mirror to adjust the simulated local laser parallel to simulated receiving laser in order to compensate the misalignment. The experiment lasts 4 h, first 2 h is for open loop and last 2 h for feedback control. The experimental data shown are analyzed in ASD, see Fig. 6. The blue dotted lines are open loop data, the black dotted lines are in-loop data, the green dots are out-of-loop data, and the red solid lines are LASD for out-of-loop data.

After the feedback control turned on, during the frequencies above 10 mHz, the residue pointing jitters of yaw and pitch motions are of $6 \text{ nrad}/\sqrt{\text{Hz}}$ and $7 \text{ nrad}/\sqrt{\text{Hz}}$, respectively, which has reached the level of eLISA's requirement.

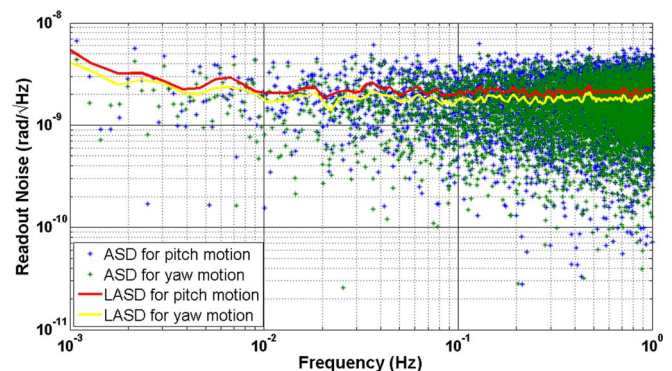


FIG. 5. Readout noise of the pointing system in pitch motion (blue points) and in yaw motion (green points) drawn in ASD, where the red curve is the LASD for pitch motion and the yellow curve is the LASD for yaw motion.

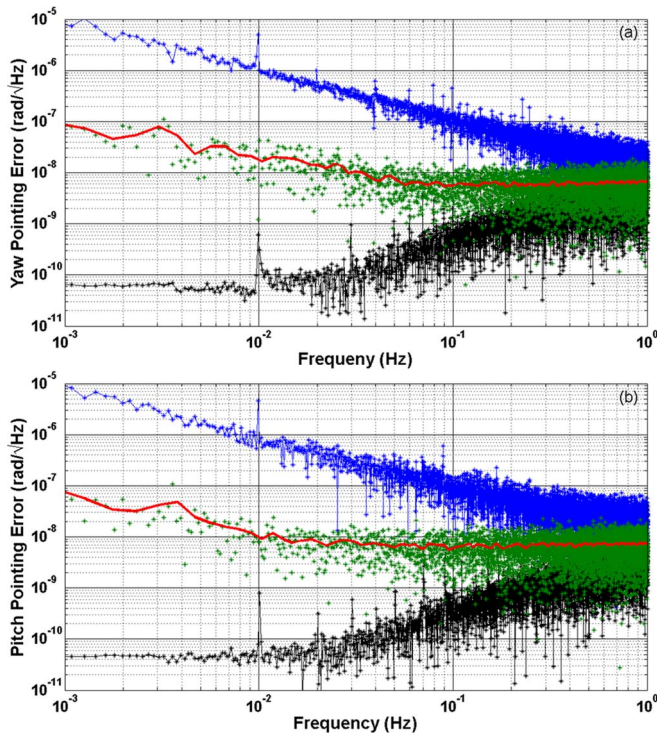


FIG. 6. (a) Results of rotating around yaw axis before control (blue points) and in control (green points) in the amplitude of $5 \mu\text{rad}/\sqrt{\text{Hz}}$; (b) results of rotating around pitch axis before control (blue points) and in control (green points) in the amplitude of $5 \mu\text{rad}/\sqrt{\text{Hz}}$. The red curves present the LASD of yaw motion or pitch motion in out-of-loop; the black dotted lines are in-loop data for yaw and pitch motion.

While in the frequency domain below 10 mHz, the residue pointing jitter noises of both direction rise up quickly and reach $100 \text{ nrad}/\sqrt{\text{Hz}}$ at 1 mHz. Furthermore, the in-loop data show that this pointing control system has the potential to reach about $1 \text{ nrad}/\sqrt{\text{Hz}}$ when the readout noise is suppressed.

V. CONCLUSIONS

A methodological demonstration of the laser beam pointing control system for space G.W. detection missions has been accomplished. The pointing jitter of $5 \mu\text{rad}$ is produced to simulate the situation of eLISA or future satellite gravity missions. With beam pointing control system turned on, the stability of the beam pointing direction can be kept at $6 \text{ nrad}/\sqrt{\text{Hz}}$ and $7 \text{ nrad}/\sqrt{\text{Hz}}$.

It is found in the experimental results that, below 10 mHz the pointing jitter noise is likely limited by thermal noise; while above 10 mHz the pointing stability is mainly restricted by the noise of electronics and the readout noise of DWS system. In the real situation of the eLISA, the receiving light will be at pW level. Therefore, shot noise dominates and greatly increases the readout noise of DWS system. The signal to noise ratio will be exceedingly reduced which will make the control of beam pointing more difficult. To design and build such a control system for pW receiving laser beam is the primary task in the following research.

ACKNOWLEDGMENTS

This work was supported by the Space Science Research Projects in Advance (SSRPA: O930143XM1) and the Scientific Equipment Development and Research Project (SEDRP: Y231411YB1) of Chinese Academy of Sciences (CAS).

- ¹K. Danzmann, P. Bender, A. Brillet, I. Ciufolini, A. M. Cruise, C. Cutler, F. Fidicaro, W. M. Folkner, J. Hough, P. McNamara *et al.*, *LISA Pre-phase A Report*, 2nd ed., Report No. MPQ 208 (Max-Planck-Institut für Quantenoptik, Garching Germany, 1998), pp. 7–34, 64–65, 81–83.
- ²O. Jennrich, P. Binetruy, M. Colpi, K. Danzmann, P. Jetzer, A. Lobo, G. Nelemans, B. Schutz, R. Stebbins, T. Sumner *et al.*, *The eLISA/NGO Whitepaper* (eLISA Working Group, 2011), pp. 5–68, 90–99.
- ³X. Gong, S. Xu, S. Bai, Z. Cao, G. Chen, Y. Chen, X. He, G. Heinzel, Y. Lau, C. Liu *et al.*, *Class. Quantum Grav.* **28**(9), 094012 (2011).
- ⁴W. T. Ni, *Int. J. Mod. Phys. D* **22**, 1341004 (2013).
- ⁵P. L. Bender, M. C. Begelman, and J. R. Gair, *Class. Quantum Grav.* **30**, 165017 (2013).
- ⁶G. M. Harry, P. Fritschel, D. A. Shaddock, W. Folkner, and E. S. Phinney, *Class. Quantum Grav.* **23**, 4887–4894 (2006).
- ⁷D. I. Robertson, P. McNamara, H. Ward, and J. Hough, *Class. Quantum Grav.* **14**, 1575–1577 (1997).
- ⁸P. L. Bender, *Class. Quantum Grav.* **22**, S339–S346 (2005).
- ⁹L. d’Arcio, J. Bogenstahl, M. Dehne, C. Diekmann, E. D. Fitzsimons, R. Fleddermann, E. Granova, G. Heinzel, H. Hogenhuis, C. J. Killow *et al.*, “Optical bench development for LISA,” in *Proceedings of the International Conference on Space Optics, Rhodes, Greece, 2010* (European Space Agency, 2010), see <http://congrex.nl/icsop/Papers/Session14b/FCXNL-10A02-2017738-1-weiseicsopaper.pdf>.
- ¹⁰M. Tinto, J. C. N. de Araujo, O. D. Aguiar, and M. E. S. Alves, *Astropart. Phys.* **48**, 50–60 (2013).
- ¹¹B. S. Sathyaprakash and B. F. Schutz, *Living Rev. Relat.* **12**, 2 (2009).
- ¹²B. F. Schutz, *Class. Quantum Grav.* **16**, A131–A156 (1999).
- ¹³C. Cutler, K. S. Thorne, L. Bildsten, A. Buonanno, C. Hogan, V. Kalogera, B. J. Owen, E. S. Phinney, T. A. Prince, F. A. Rasio *et al.*, in *Proceedings of the GR16 Conference on General Relativity and Gravitation* (World Scientific, Singapore, 2002), pp. 72–111.
- ¹⁴K. Danzmann, P. A. Seoane, S. Aoudia, G. Auger, S. Babak, E. Barausse, M. Bassan, V. Beckmann, P. Bineruy, J. Bogenstahl *et al.*, *eLISA Whitepaper-RC1* (eLISA Working Group, 2013), pp. 13–14.
- ¹⁵P. Amaro-Seoane, S. Aoudia, S. Babak, P. Binetruy, E. Beriti, A. Bohé, C. Caprini, M. Colpi, N. J. Cornish, K. Danzmann *et al.*, *Class. Quantum Grav.* **29**, 124016 (2012).
- ¹⁶B. L. Schumaker, *Class. Quantum Grav.* **20**, S239–S253 (2003).
- ¹⁷F. Antonucci, M. Armano, H. Audley, G. Auger, M. Benedetti, P. Binetruy, C. Boatella, J. Bogenstahl, D. Bortoluzzi, P. Bosetti *et al.*, *Class. Quantum Grav.* **28**, 094002 (2011).
- ¹⁸D. Z. Anderson, *Appl. Opt.* **23**, 2944–2949 (1984).
- ¹⁹E. Morrison, B. J. Meers, D. I. Robertson, and H. Ward, *Appl. Opt.* **33**, 5041–5049 (1994).
- ²⁰E. Morrison, B. J. Meers, D. I. Robertson, and H. Ward, *Appl. Opt.* **33**, 5037–5040 (1994).
- ²¹G. Heinzel, A. Rüdiger, R. Schilling, K. Strain, W. Winkler, J. Mizuno, and K. Danzmann, *Opt. Commun.* **160**, 321–334 (1999).
- ²²G. Heinzel, C. Braxmaier, R. Schilling, A. Rüdiger, D. Robertson, M. T. Plate, V. Wand, K. Arai, U. Johann, and K. Danzmann, *Class. Quantum Grav.* **20**, S153–S161 (2003).
- ²³G. Heinzel, V. Wand, A. García, O. Jennrich, C. Braxmaier, D. Robertson, K. Middleton, D. Hoyland, A. Rüdiger, R. Schilling, U. Johann, and K. Danzmann, *Class. Quantum Grav.* **21**, S581–S587 (2004).
- ²⁴H. S. Liu, Y. H. Dong, Y. Q. Li, Z. R. Luo, and G. Jin, *Rev. Sci. Instrum.* **85**, 024503 (2014).
- ²⁵Y. Q. Li, Z. R. Luo, H. S. Liu, Y. H. Dong, and G. Jin, *Chin. Phys. Lett.* **29**, 079501 (2012).
- ²⁶F. Cirillo and P. F. Gath, *J. Phys. Conf. Ser.* **154**, 012014 (2009).
- ²⁷B. Sheard, G. Hezel, K. Danzmann, D. A. Shaddock, W. M. Klipstein, and W. M. Folkner, *J. Geodesy* **86**, 1083–1095 (2012).
- ²⁸I. Panet, J. Flury, R. Biancale, T. Gruber, J. Johannessen, M. R. van den Broeke, T. van Dam, P. Gegout, C. W. Hughes, G. Ramillien, I. Sasgen, L. Seoane, and M. Thomas, *Surv. Geophys.* **34**, 141–163 (2013).

- ²⁹G. Heinzel, B. Sheard, N. Brause, K. Danzmann, M. Dehne, O. Gerberding, C. Mahrtd, V. Müller, D. Schütze, G. Stede, W. Klipsteiny, W. Folknery, R. Speroy, K. Nicklausz, P. Gathx, and D. Shaddock, "Laser ranging interferometer for GRACE follow-on," in *Proceedings of the International Conference on Space Optics, Ajaccio, Corse, France, 2012* (the Centre National d'Etudes Spatiales (CNES), 2012), p. 062.
- ³⁰D. Schütze, G. Stede, V. Müller, O. Gerberding, C. Mahrtd, B. Shead, G. Heinzel, and K. Danzmann, *ASP Conf. Ser.* **467**, 285–289 (2013).
- ³¹B. D. Loomis, R. S. Nerem, and S. B. Luthcke, *J. Geodesy* **86**, 319–335 (2012).
- ³²M. Tröbs and G. Heinzel, *Measurement* **39**(2), 120–129 (2006).